Acta Neuropathol (2001) 101 : 27–35
DOI 10.1007/s004010000256

REGULAR PAPER

**Akinori Takeda · Masakazu Wakai · Hisayoshi Niwa
Rika Dei · Masahiko Yamamoto · Mei Li · Yoji Goto
Takeshi Yasuda · Yuji Nakagomi · Masaki Watanabe
Toshiaki Inagaki · Yoshinari Yasuda · Toshio Miyata
Gen Sobue**

Neuronal and glial advanced glycation end product [N^{ε}-(carboxymethyl)lysine] in Alzheimer's disease brains

Received: 14 January 2000 / Revised: 8 March 2000, 2 May 2000 / Accepted: 2 May 2000 / Published online: 5 September 2000

Abstract The cellular distribution of an advanced glycation end product [N^{ε}-(carboxymethyl)lysine (CML)] in aged and Alzheimer's disease (AD) brains was assessed immunohistochemically. CML was localized in the cytoplasm of neurons, astrocytes, and microglia in both aged and AD brains. Glial deposition was far more marked in AD brains than in aged brains, and neuronal deposition was also increased. On electron microscopic immunohistochemistry, neuronal CML formed granular or linear deposits associated with lipofuscin, and glial deposits formed lines around the vacuoles. Neuronal and glial deposits were prominent throughout the cerebral cortex and hippocampus, but were sparse in the putamen, globus pallidus, substantia nigra, and cerebellum, with glial deposits being far more prominent in AD brains. The distribution of neuronal and glial deposits did not correspond with the distribution of AD pathology. The extent of CML deposits was inversely correlated with neurofibrillary tangle formation, particularly in the hippocampus. Most hippocampal pyramidal neurons with neurofibrillary tangles did not have CML, and most of the neurons with heavy CML deposits did not have neurofibrillary tangles. In the hippocampus, neuronal CML was prominent in the region where neuronal loss was mild. These observations suggest that CML deposition does not directly cause neurofibrillary tangle formation or neuronal loss in AD.

Key words Advanced glycation end products · N^{ε}-(Carboxymethyl)lysine · Astrocyte · Microglia · Oxidative stress

A. Takeda · M. Wakai · H. Niwa · R. Dei · M. Yamamoto
M. Li · Y. Goto · T. Yasuda · Y. Yasuda · G. Sobue (✉)
Department of Neurology,
Nagoya University School of Medicine,
Tsurumai 65, Showa, Nagoya 466-8550, Japan
e-mail: sobueg@tsuru.med.nagoya-u.ac.jp,
Tel.: +81-52-7442385, Fax: +81-52-7442384

A. Takeda · Y. Goto
Department of Neurology, Oyamada Memorial Spa Hospital,
Yokkaichi, Japan

Y. Nakagomi
Laboratory of Electron Microscopy, Aichi Medical University,
Aichi, Japan

M. Watanabe
Department of Neurology, Nagoya First Red Cross Hospital,
Nagoya, Japan

T. Inagaki
Department of Internal Medicine,
Nagoya City Kouseiin Geriatric Hospital, Nagoya, Japan

Y. Yasuda · T. Miyata
Institute of Medical Science and Department of Medicine,
Tokai University, Kanagawa, Japan

Introduction

Non-enzymatic glycation and oxidation of proteins and lipids by aldose sugars produces advanced glycation end products (AGEs). AGEs are known to occur in tissue proteins and lipids with a slow turnover in the elderly [1, 2]. AGE formation is usually a slow process that occurs through Amadori intermediate products, but is significantly accelerated in pathological conditions by the presence of active oxygen radicals, carbonyl compounds and other reactive molecules [3, 4, 5]. AGE accumulation is prominent in patients with diabetes mellitus, arteriosclerosis, and uremia [6, 7, 8, 9], in which the levels of oxygen radicals and carbonyl compounds are known to be elevated [10, 11, 12]. Recently, AGEs have been shown to accumulate in both aged and Alzheimer's disease (AD) brains, and have been suggested to play a role in the aging process as well as in the pathogenesis of AD [13, 14, 15, 16, 17, 18, 19, 20, 21, 22].

However, it is still controversial whether AGEs actually play a role in AD. AGE-modified Aβ protein has been shown to accelerate the aggregation of soluble Aβ in vitro, and the plaque fraction of AD brains has also been shown to contain increased amounts of AGE adducts [15]. In addition, AGE-modified recombinant tau protein has been shown to generate reactive oxygen intermediates [16]. Furthermore, pentosidine and pyrraline, two epitopes

of AGEs, were demonstrated to co-localize with senile plaques and neurofibrillary tangles (NFTs) in AD brains [17]. Recently, it was documented that a receptor for AGEs (RAGE) is also a specific cell-surface acceptor for Aβ, and that RAGE is involved in Aβ-mediated toxicity for neuronal cells [21]. In contrast, it has also been proposed that glycation of Aβ is a late event in the evolution of AD pathology and that it results from free radical generation by Aβ itself [23]. In addition, it was demonstrated that Aβ toxicity does not require RAGE protein [24].

In this study, we assessed the tissue distribution of an AGE epitope, N^{ε}-(carboxymethyl)lysine (CML), in aged and AD brains, and also investigated the correlation between AGE accumulation and AD pathology.

Materials and methods

Brain tissues were obtained from 20 patients with clinicopathologically confirmed AD (age range: 80–85 years), 21 age-matched control patients without dementia (age range: 73–92 years), and two young males (15 and 17 years old) who died of non-neurological diseases. Various brain regions were fixed in 10% buffered formalin and embedded in paraffin. The AD patients had a history of Alzheimer-type dementia with a well-documented duration of disease, and also had a confirmed neuropathological diagnosis of AD. Their brains showed no evidence of vascular insults, cortical Lewy bodies, or lesions suggesting any other neurological disorder. Autopsy was performed within 8 h of death.

Antibodies

Two antibodies were used for detection of CML. One was a rabbit polyclonal anti-AGE IgG, the major epitope of which have been reported to be CML previously [8, 9, 18]. Another was a mouse monoclonal anti-AGE IgG (6D12, Wako Pure Chemicals, Osaka, Japan) targeting CML, the characteristics of which have been described previously [25, 26, 27]. A rabbit anti-human tau antibody (Dako, Glostrup, Denmark), a monoclonal anti-human glial fibrillary acidic protein (GFAP) antibody (6F2, Dako), and a monoclonal anti-human pan-macrophage antibody (Ki-M1p, IV-20, Seikagaku Kogyo, Tokyo, Japan) were also used.

Light and electron microscopic immunohistochemistry

Serial sections (4 μm thick) were deparaffinized and rehydrated. Sections for detection of CML were heated in a microwave oven for 15 min. All sections were incubated with 0.3% H_2O_2 in methanol for 30 min, blocked with diluted normal goat or horse serum, and then incubated with anti-AGE antibody (0.5 mg/ml) or anti-human tau rabbit antibody (diluted to 1:100) in a humid chamber for 2 h at room temperature. Detection was performed using an ABC staining kit (Vectastain, Burlingame, Calif.) according to the manufacturer's protocol.

For electron microscopic immunohistochemistry, buffered formalin-fixed, paraffin-embedded tissue sections were immunostained with antibodies for CML, and then incubated with a horseradish peroxidase-labeled secondary antibody (Amersham, Buckinghamshire, UK). The tissue sections were then visualized with 3,3'-diaminobenzidine tetrahydrochloride (Dako), fixed with 2% osmium tetroxide in 0.1 M phosphate buffer (pH 7.4), dehydrated in an alcohol series, and embedded in epoxy resin. Ultrathin sections were cut and observed under an electron microscope (Hitachi H-7000, Tokyo, Japan) [28, 29].

Double-labeling immunohistochemistry was performed with two primary antibodies (anti-human GFAP/anti-CML or anti-human pan-macrophage/anti-CML). Monoclonal anti-human GFAP antibody was diluted to 1:200, and monoclonal anti-human pan-macrophage antibody was diluted to 1:100. Sections for the pan-macrophage immunoreaction were pretreated with 0.1% trypsin for 15 min at 37°C as described previously [20]. All sections were preincubated with 3% H_2O_2 in water and then with normal swine serum diluted in 0.05 M TRIS buffer (pH 7.6) containing bovine serum albumin. Subsequently, incubation was performed with the two primary antibodies diluted in TRIS-buffered saline (0.05 M TRIS, 0.15 M NaCl, pH 7.6) for 2 h at room temperature. Detection was performed using a Dako double staining kit according to the manufacturer's protocol.

Assessment of the tissue distribution of CML and AD pathology

In the hippocampus and the third layer of the inferior temporal cortex, CML immunoreactivity and AD pathology were quantified and correlated. The frequency of CML-positive neurons was calculated by examining at least 200 pyramidal cells in the CA1, 2, 3 and 4 regions of the hippocampus and the neurons in the third layer of the inferior temporal cortex. CML-positive vesicles and vacuoles associated with glial cells in the neuropil were counted in three randomly selected areas in each target region. The loss of pyramidal neurons in the hippocampus and the intracellular NFT formation were assessed using the adjacent sections to those used for detection of CML. The loss of pyramidal neurons was estimated semiquantitatively, and graded as – (negative), ± (mild loss), + (moderate loss) or ++ (severe loss). The NFT formation by pyramidal neurons was quantitatively assessed using staining with anti-human tau antibody and the methenamine silver method of sections that were adjacent to those employed to assess CML deposition. The NFT formation was expressed as the number per 1 mm^2 area of the CA1, 2, 3 and 4 regions. Moreover, hippocampal pyramidal neurons were assessed on at least 200 pyramidal neurons as to whether they had CML, NFTs, both or neither in three randomly selected areas in the CA1, 2, 3 and 4 regions, using adjacent sections.

The tissue distribution of CML in various regions of the whole brain was semiquantitatively assessed by scoring the CML immunoreactivity. The percentage of CML-positive neurons was assessed by examining at least 200 neurons with obvious nucleoli in each target area, and was classified as 0 (negative or mildly positive: less than 20% of neurons were positive), +1 (moderately positive: between 20% and 70%), or +2 (strongly positive: more than 70%). The immunoreactivity of CML in the extra-neuroperikarya was estimated by counting CML-positive vesicles and vacuoles in the neuropil from at least three randomly selected areas (1 mm^2), and was classified as 0 (negative or mildly positive: less than 50 CML-positive deposits), +1 (moderately positive: between 50 and 100), or +2 (strongly positive: more than 100).

Data are expressed as the mean ± SD. The Mann-Whitney U-test was used for the statistical comparison of two groups. Significance was defined when the P value was less than 0.05.

Results

CML immunoreactivity (neuronal and glial CML) in aged and AD brains

In the neurons of AD brains, CML immunoreactivity was granular and was found in the cytoplasm adjacent to the nucleus. This pattern was designated as neuronal CML (Fig. 1A). Neuronal CML was not detected inside the nucleus. CML immunoreactivity was also prominent in the extra-neuroperikaryal space of the neuropil. The extra-neuroperikaryal CML immunoreactivity was more coarsely granular and vesicular than neuronal CML, resembling aggregates of CML-positive vacuoles of various sizes. In aged brains, we detected a similar pattern of neuronal

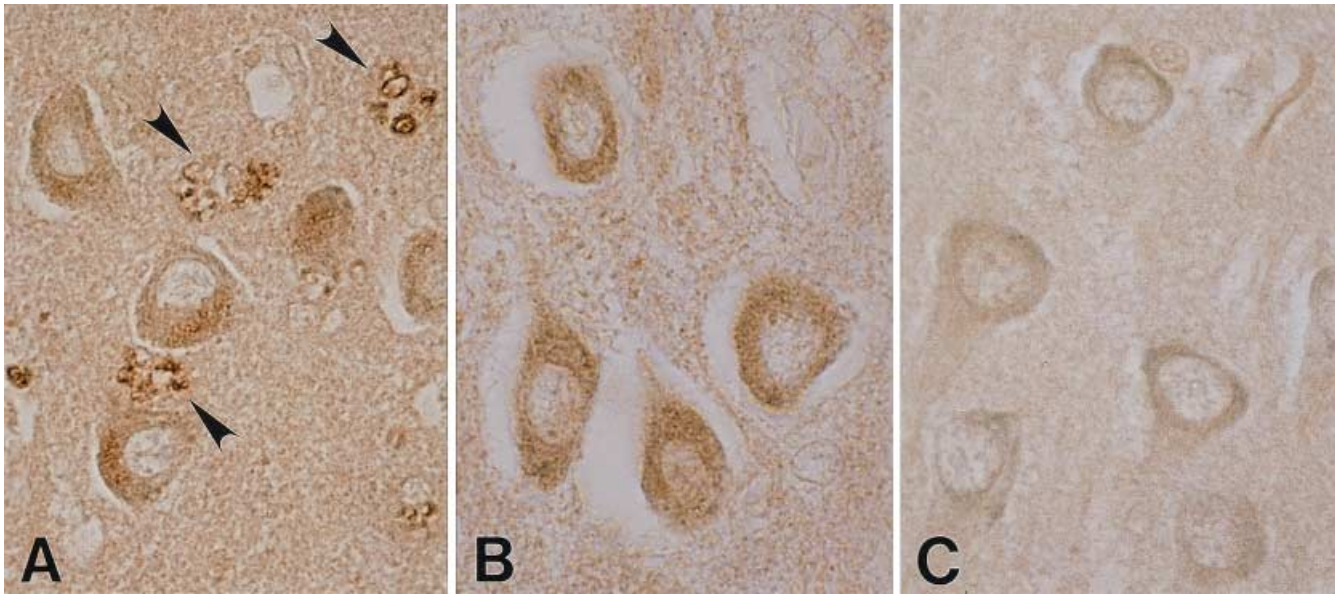

Fig. 1A–C Immunohistochemical detection of CML in the hippocampus (CA4). **A** In an AD brain, the neurons showed microgranular CML immunoreactivity (neuronal CML), and coarser granular and vesicular CML immunoreactivity was seen in the neuropil (glial CML, *arrowhead*). **B** In a normal aged brain, the neurons showed similar CML immunoreactivity, but few glial CML immunoreactivity. **C** In a young brain, CML staining was undetectable [*AD* Alzheimer's disease, *CML* N^{ε}-(carboxymethyl)lysine]. **A–C** ×360

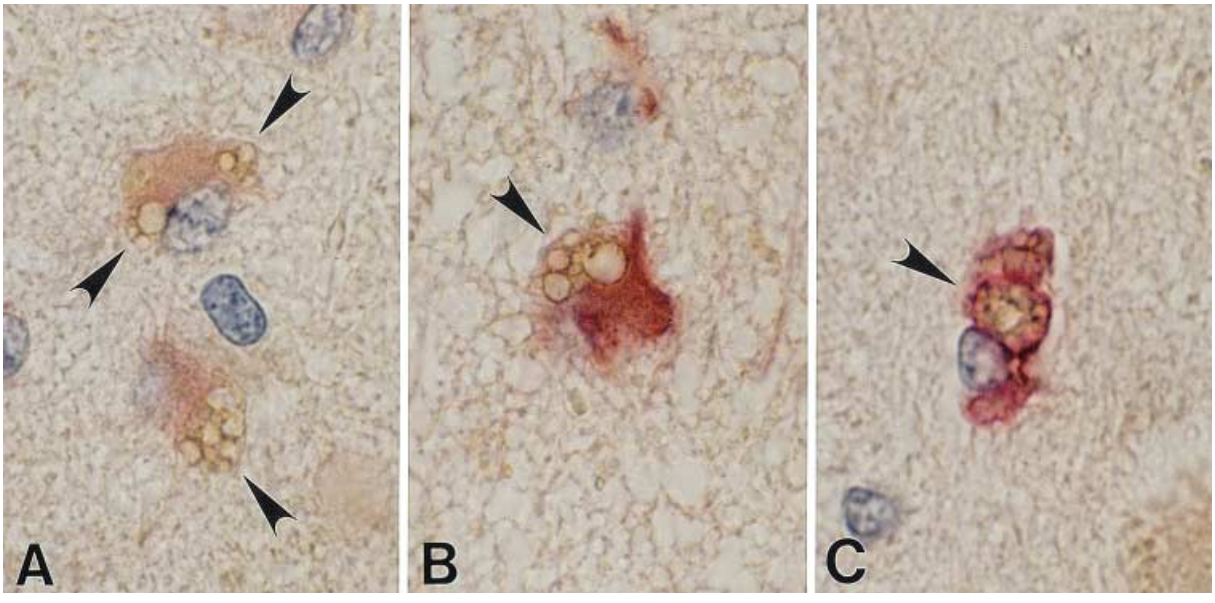

Fig. 2A–C Co-localization of CML with astrocytes or microglia. Double immunolabeling of the hippocampus of AD brains with anti-GFAP/anti-CML (**A**,**B**) and anti-human pan-macrophage/anti-CML (**C**). Most extra-neuroperikaryal CML aggregates (*brown*, *arrowhead*) were co-localized in GFAP-positive astrocytes (*red*) (**A**,**B**), while some CML aggregates (*brown*, *arrowhead*) in the neuropil were co-localized with microglia (**C**). **A**,**B** ×400; **C** ×600

CML, but extra-neuroperikaryal CML was extremely rare when compared with AD brains (Fig. 1B). CML was almost undetectable in young brains (Fig. 1C). Blocking of anti-CML antibody with AGE-bovine serum albumin or synthesized CML-bovine serum albumin dramatically reduced immunostaining in both aged and AD brains (data not shown).

The double-labeling study combined marker antibodies for astrocytes (anti-GFAP antibody) and microglia (anti-pan-macrophage antibody) with anti-CML antibodies. It clearly demonstrated that extra-neuroperikaryal CML immunoreactivity was localized in the cytoplasm of astrocytes and microglia, with this pattern being designated as glial CML (Fig. 2A, B).

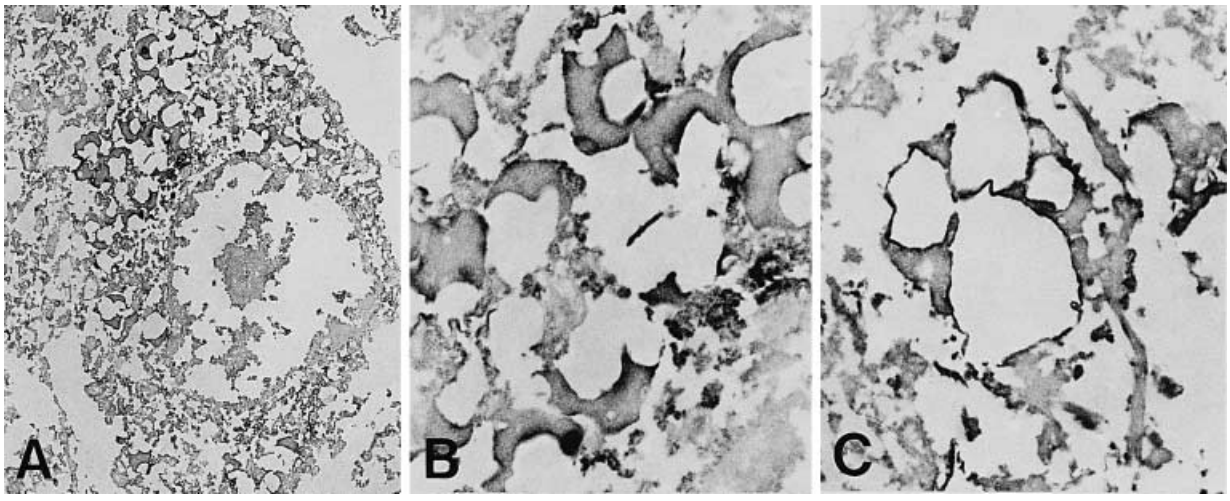

Fig. 3A–C Electron microscopic CML immunohistochemistry in an AD brain. Intraneuronal CML immunoreactivity was mainly located in the lipofuscin complex, especially forming a cap-like, linear arrangement (**A**,**B**). Vacuolated lipid droplets were negative. The extra-neuroperikaryal CML immunoreactivity was both linear and cap-like around vacuolated structures that were probably lipid droplets (**C**). **A** ×2,000; **B**,**C** ×6,000

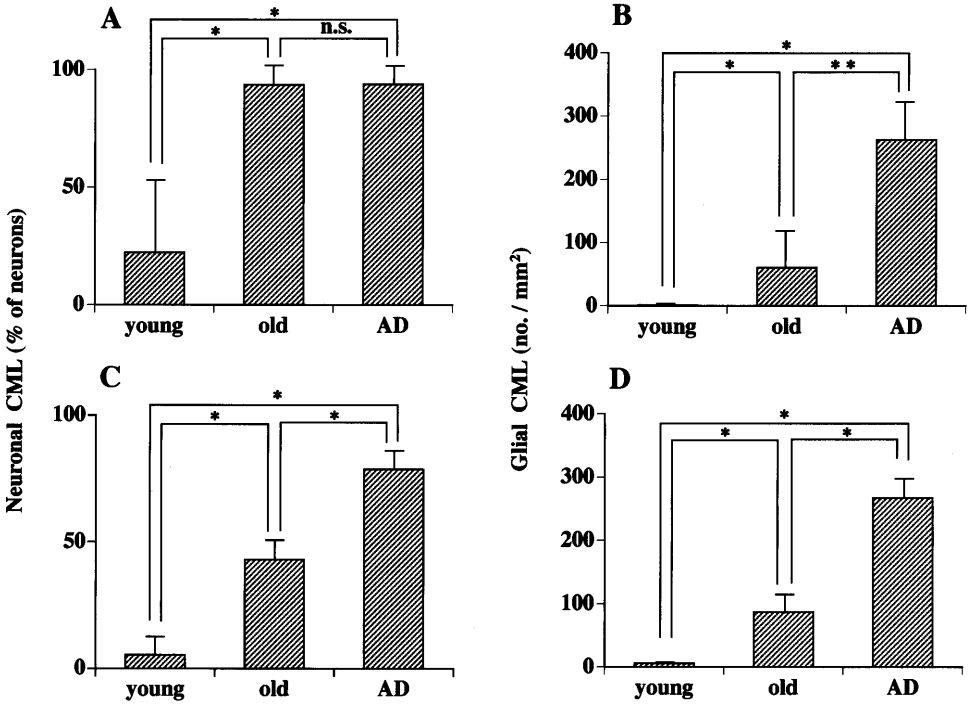

Fig. 4A–D CML immunoreactivity in young, old, and AD brains. The frequency of CML-positive pyramidal neurons (neuronal CML) in the CA4 (**A**) and the inferior temporal cortex (**C**). The number of glial CML deposits was counted in three randomly selected areas of 1 mm^2 in the CA4 (**B**) and inferior temporal cortex (**D**). * and ** denote $P<0.05$ and $P<0.01$, respectively. In AD brains, neuronal CML was almost similar or slightly more prominent than in age-matched control brains, but glial CML was far more prominent in AD brains

Electron microscopic immunohistochemistry showed that neuronal CML immunoreactivity formed a cap-like linear arrangement in the lipofuscin complex (Fig. 3A, B). Small granular CML-positive aggregates were also present in the neuronal cytoplasm (Fig. 3A, B). Glial CML immunoreactivity formed a line around vacuolated structures that were probably lipid droplets (Fig. 3C).

These findings indicated that CML immunoreactivity occurred in the cytoplasm of glial cells in AD, with such cells being prominent in AD brains.

Expression and tissue distribution of CML immunoreactivity in aged and AD brains

Quantitative assessment of CML immunoreactivity in the CA4 region of the hippocampus demonstrated that the CML-positive pyramidal neurons population were significantly increased in both aged and AD brains when compared with young brains ($P<0.05$), but were similar in aged and AD brains (Fig. 4A). However, glial CML immunoreactivity was significantly more common in AD

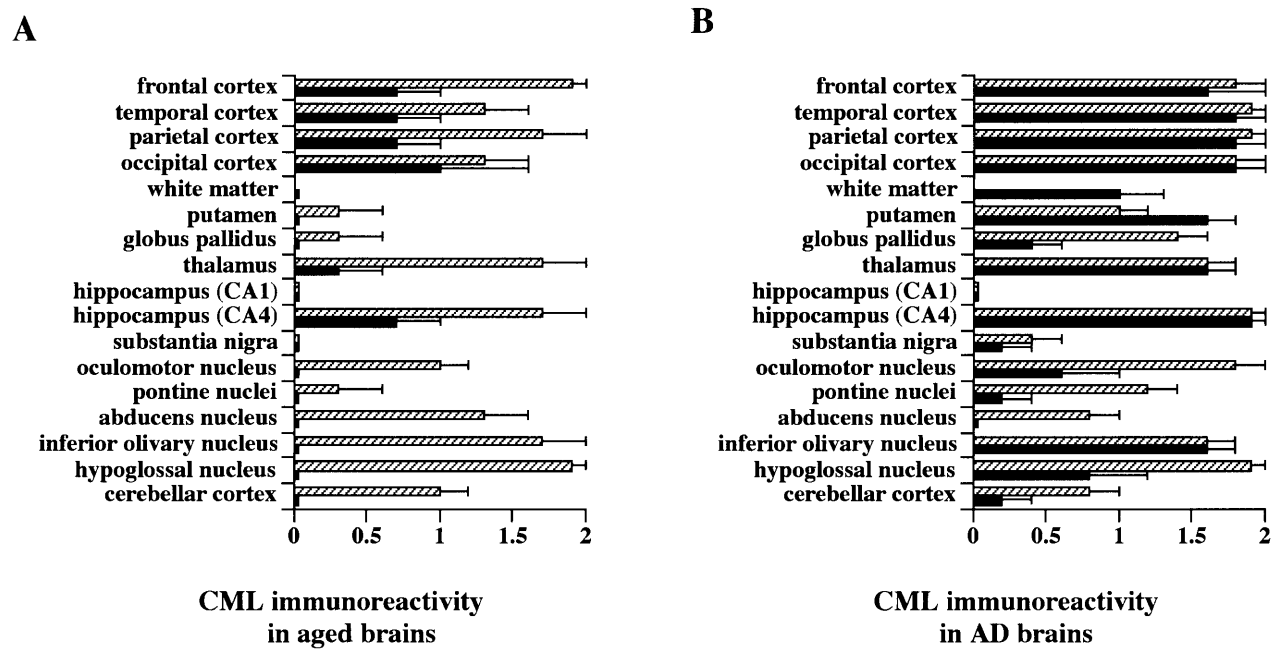

Fig. 5A,B Tissue distribution of neuronal and glial CML in aged and AD brains. Neuronal and glial CML immunoreactivity were graded as *0* (negative or mildly positive), *+1* (moderately positive), and *+2* (strongly positive). The mean and SD are shown for the aged brains (**A**) and AD brains (**B**). The *hatched bars* show neuronal CML and the *closed bars* show glial CML

brains than in aged brains ($P<0.01$) (Fig. 4B). In the third layer of the inferior temporal gyrus, neuronal CML was significantly more common in AD brains compared with both young brains ($P<0.05$) and aged brains ($P<0.05$) (Fig. 4C). The number of glial CML structures was significantly higher in AD brains compared with both young brains ($P<0.05$) and aged brains ($P<0.05$) (Fig. 4D).

The tissue distribution of CML immunoreactivity in the brain is summarized in Fig. 5. In aged brains, neuronal CML was prominent in the cerebral cortex, including the CA4 region of the hippocampus and some brain stem nuclei, but was rare in the CA1 region of the hippocampus, and in the putamen, globus pallidus, substantia nigra, some brain stem nuclei, and the cerebellar cortex. Glial CML generally showed low levels of staining in aged brains (Fig. 5A). In AD brains, however, both neuronal and glial CML was prominent throughout the brain, except for the hippocampus (CA1), some brain stem nuclei and the substantia nigra (Fig. 5B).

CML, neurofibrillary tangles, and neuronal loss in the hippocampus of AD brains

In the CA4 region of AD brains, there were prominent neuronal and glial CML deposits, but NFT formation and loss of pyramidal neurons were very mild (Table 1). On the contrary, in the CA1 region of AD brains, neuronal and glial CML deposits were significantly less prominent than in the CA4 ($P<0.001$), whereas NFT formation and pyramidal neuronal loss were more marked (Table 1). CML deposits, NFT formation, and pyramidal neuronal loss in the CA2 and CA3 regions were intermediate between the changes in CA1 and CA4 (Table 1). Consecutive sections

Table 1 CML immunoreactivity, NFT formation and pyramidal neuron loss in the hippocampus of AD brains. The frequency of CML-positive neurons were assessed for 200–500 pyramidal neurons in each region. Glial CML and NFTs were estimated by counting in 1 mm^2 areas. The loss of pyramidal neurons was estimated semiquantitatively and graded as: – (negative), ± (mild loss), + (moderate loss), and ++ (severe loss). Statistical analysis was performed to compare the CA1 and CA4 regions by Mann-Whitney U-test. In the CA1 region of AD brains, there were significantly fewer neuronal CML deposits, fewer glial CML deposits, and more NFTs than in the CA4 region. The CA2 and CA3 regions were intermediate between the CA1 and CA4 regions. Neuronal loss was severe in the CA1 region and negative in the CA4 region

CML and AD pathology	Region of hippocampus				*P* value (CA1 vs CA4)
	CA1	CA2	CA3	CA4	
Neuronal CML (%)	17.6±15.9	43.3±30.5	85.7±21.2	94.5± 5.5	<0.001
Glial CML (no./mm^2)	39.9±22.8	70.2±38.4	141.9±58.5	219.0±65.4	<0.001
NFTs (no./mm^2)	93.0±51.6	45.6±39.3	5.4± 7.5	3.9± 6.3	<0.001
Neuronal loss	++	+	±~–	–	

Table 2 Average frequency of pyramidal neurons with CML and/or tau in the hippocampus of AD brains. The frequency of CML positive or negative, tau-positive or negative neurons were assessed for 200–500 pyramidal neurons in each region. The frequency of neurons with both CML and tau were from 1.5% to 4.9%. Statistical analysis was performed to compare the CA1 and CA4 regions by Mann-Whitney U-test

	Region of hippocampus				*P* value (CA1 vs CA4)
	CA1	CA2	CA3	CA4	
CML-positive, tau-positive neurons (%)	2.9± 5.1	4.9± 7.4	1.5± 1.4	2.0±3.3	n.s.
CML-positive, tau-negative neurons (%)	17.1±15.6	36.0±19.2	82.4±18.4	87.6±9.7	<0.005
CML-negative, tau-positive neurons (%)	44.8±33.3	18.7±19.9	7.9± 9.7	3.7±4.3	<0.005
CML-negative, tau-negative neurons (%)	35.2±20.2	40.3± 6.8	7.9± 7.4	6.3±7.4	<0.05

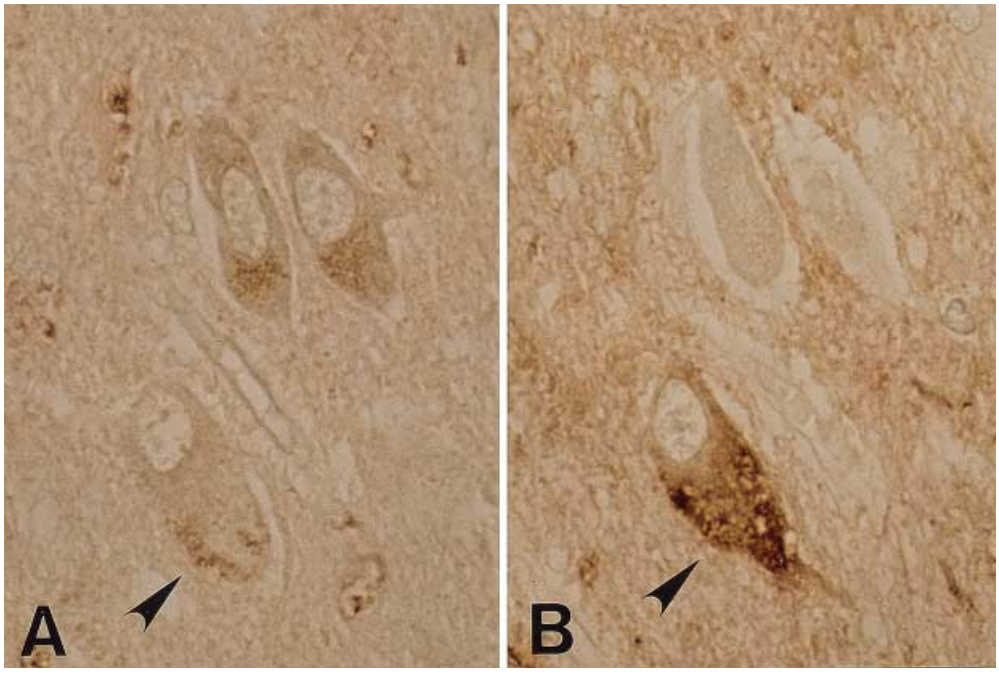

Fig. 6 Adjacent sections of the hippocampus from an AD brain stained for CML immunoreactivity (**A**) and for tau immunoreactivity (**B**). Only a few neurons were positive for both tau immunoreactivity and CML immunoreactivity (*arrowhead*). **A**,**B**, ×400

stained with anti-CML antibody and anti-human tau antibody showed that the majority of the pyramidal neurons with neuronal CML deposits had no immunoreactivity for tau, and vice versa. There were only a few neurons that showed co-localization of CML deposits and tau-positive NFTs (Table 2, Fig. 6A, B).

Discussion

In this study, we demonstrated that CML deposits occurred in the neuronal cytoplasm as well as in the cytoplasm of astrocytes and microglia, and that these deposits were more prominent in AD brains than in age-matched control brains to a varying extent depending on the brain region. The increase of neuronal CML deposits was significant in some regions of AD brains, while glial CML was generally far more prominent in AD brains than in aged brains. In other words, neuronal CML deposition was significantly increased in the temporal and occipital cortex and in some brain stem nuclei of AD brains, whereas glial CML deposition was far more marked in most regions of AD brains than in aged brains. These results indicate that CML deposition is far greater in AD brains than in aged brains, with the increase being more prominent for glial CML than neuronal CML.

The question is, therefore, raised as to why glial CML is markedly increased in AD brains. One possibility is that glial CML is derived from neuronal CML that is released through neuronal degeneration and death and is subsequently endocytosed by microglia and astroglia. However, the electron microscopic features of glial CML were not those of endocytosomes (Fig. 3C), and glial CML was also prominent in the regions without marked neuronal loss, suggesting that accumulation of glial CML is not secondary to neuronal loss. Recently, it was found that the formation of AGEs is accelerated in pathological conditions associated with increased levels of oxygen radicals, carbonyl compounds, or other reactive molecules [3, 4, 5]. Carbonyl compounds and various oxygen radicals have been demonstrated to be increased in the AD brains [30, 31, 32]. Thus, glial CML could be primarily synthesized in the glial cytoplasm as a result of the elevated levels of carbonyl compounds and oxygen radicals in AD brains.

Neuronal CML deposits were prominent even in the normal aged brains, although deposition was greater in AD to some extent. These observations may suggest that conditions promoting CML formation may initially increase CML deposits in neurons and that more extreme conditions may increase glial CML in AD brains.

Nowadays astrocytes are found to be more resistant to oxygen radicals and to play a protective role for neurons and oligodendrocytes [33, 34, 35]. For example, co-culture with astrocytes attenuates killing by H_2O_2 of striatal neurons [34], and astrocytes exposed to low levels of H_2O_2 increase neuroprotective proteins such as nerve growth factor and basic fibroblast growth factor [35]. In the present study, in many regions of AD brains neurons with CML were accompanied by astrocytes with CML. In the CA4 region of AD brains many astrocytes with CML were prominent and neuronal loss was not so marked, whereas in the CA1 region there were few astrocytes with CML and marked neuronal loss. CML-bearing astrocytes may be protecting neurons against oxidative stress.

Another striking observation in this study was a relation between neuronal CML deposition and AD pathology in AD brains. Particularly in the CA1 and CA4 regions of the hippocampus, the extent of neuronal CML deposition seemed to have an inverse correlation with pyramidal neuronal loss. In the regions where neuronal loss was severe, CML deposition was less prominent, and vice versa. What causes the difference of neuronal CML formation between in the CA1 and CA4 region? There may be that CA1 neurons which had formed CML soon died, and that, therefore, few CA1 neurons with CML were detected. However, in aged brains with less neuronal loss, the difference of neuronal CML deposits between in the CA1 and CA4 regions was present, as shown in the present study and a previous study [14]. Another possibility is that it may result from a difference in oxidative stress level between these regions. However, it has been reported that 4-hydroxynoneal adducts, the potent neurotoxic product of lipid peroxidation, were present in CA1 neurons as much as in CA4 neurons of AD brains [36]. It means that oxidative stress is present not only in the CA4 region but also in the CA1 region. It is also possible that the difference in CML formation in CA1 and CA4 neurons may arise from the differences in the properties of these neurons. Moreover, the neurons which form CML may be more resistant to oxidative stress than the neurons which do not form CML. Some AGEs have been shown to play a direct role in cell damage under conditions which promote oxygen radicals [37], but the oxidative and carbonyl stresses that accelerate AGE formation are thought to be far stronger toxic factors than AGEs themselves [38, 39].

In the present study, only a few tau-positive neurons were also positive for CML immunoreactivity and vice versa. This result is not consistent with the report that NFTs were stained with anti-AGE antibody [17]. On the other hand, Sasaki et al. [22] reported that approximately 20% of intracellular NFTs were stained with anti-AGE antibody. These differences may come from the differences of antibodies used. In other words, our antibodies recognized CML among AGEs, and the antibodies used in the study by Smith et al. [17] were shown to react with pyrraline or pentosidine.

Stojanovic et al. [40] demonstrated an inverse relationship between the amount of lipofuscin and NFTs, and suggested that the small amount of lipofuscin pigment in NFT-bearing neurons reflected their inability to store toxic metabolic byproducts of the oxidative process. In our study, neuronal CML was co-localized with lipofuscin pigment in aged and AD brains according to electron microscopic immunohistochemistry, an observation in agreement with previous light microscopic studies [19, 27]. Lipofuscin is an intracellular fluorescent pigment generated during the oxidation of membrane-bound insoluble proteins, lipids, and carbohydrates, which accumulates with aging, and cannot be further degraded [41]. CML has also been found to be a product of lipid peroxidation, as well as glycoxidation [42]. Thus, most of the physicochemical properties of lipofuscin pigments are common to those of CML. The neurons with a larger amount of lipofuscin and CML may scavenge oxidative stress by forming lipofuscin and CML, and may thus be protected against NFT formation and neuronal loss.

Recently, Lewy bodies in Parkinson's disease, Hirano bodies in AD and neuronal and glial hyaline inclusions in familial amyotrophic lateral sclerosis with mutant superoxide dismutase have been shown to be heavily AGE-modified [43, 44, 45, 46]. Modification by AGEs is currently considered to be neurotoxic. AGE modification of certain proteins may be related to scavenging of cytotoxic radicals and may thus provide a protective effect against neuronal degeneration in the AD brain. Taken together, we speculate that AGE formation may not be only the hallmark of oxidative or carbonyl stress which the tissue received but also the hallmark of protective function against oxidative stress.

Acknowledgments We are grateful to Ms. Sugiko Yokoi for her excellent technical assistance. This work was supported by a COE grant from the Ministry of Science, Culture and Education of Japan, and by grants from the Ministry of Health and Welfare of Japan.

References

1. Dyer DG, Dunn JA, Thorpe SR, Bailie KE, Lyons TJ, McCance DR, Baynes JW (1993) Accumulation of Maillard reaction products in skin collagen in diabetes and aging. J Clin Invest 91: 2463–2469
2. Araki N, Ueno N, Cakrabarti B, Morino Y, Horiuchi S (1992) Immunohistochemical evidence for the presence of advanced glycation end products in human lens proteins and its positive correlation with aging. J Biol Chem 267: 10211–10214
3. Glomb MA, Monnier VM (1995) Mechanism of protein modification by glyoxal and glycoaldehyde, reactive intermediate of Maillard reaction. J Biol Chem 270: 10017–10026
4. Hamada Y, Araki N, Kou N, Nakamura J, Horiuchi S, Hotta N (1996) Rapid formation of advanced glycation end products by intermediate metabolites of glycolytic pathway and polyol pathway. Biochem Biophys Res Commun 228: 539–543

5. Niwa H, Takeda A, Wakai M, Miyata T, Yasuda Y, Mitsuma T, Kurokawa K, Sobue G (1998) Accelerated formation of *N*ε-(carboxymethyl) lysine, an advanced glycation end product, by glyoxal and 3-deoxyglucosone in cultured rat sensory neurons. Biochem Biophys Res Commun 248: 93–97
6. Brownlee M, Cerami A, Vlassara H (1988) Advanced glycosylation end products in tissue and the biochemical basis of diabetic complications. N Engl J Med 318: 1315–1321
7. Nakamura Y, Horii Y, Nishino T, Shiki H, Sakaguchi Y, Kagoshima T, Dohi K, Makita Z, Vlassara H, Bucala R (1993) Immunohistochemical localization of advanced glycosylation end products in coronary atheroma and cardiac tissue in diabetes mellitus. Am J Pathol 143: 1649–1656
8. Miyata T, Oda O, Inagi R, Iida Y, Araki N, Yamada N, Horiuchi S, Taniguchi N, Maeda K, Kinoshita T (1993) β2-microglobulin modified with advanced glycation end products is a major component of hemodialysis-associated amyloidosis. J Biol Chem 92: 1243–1252
9. Miyata T, Taneda S, Kawai R, Ueda Y, Horiuchi S, Hara M, Maeda K, Monnier VM (1996) Identification of pentosidine as a native structure for advanced glycation end products in β2-microglobulin-containing amyloid fibrils in patients with dialysis-related amyloidosis. Proc Natl Acad Sci USA 93: 2353–2358
10. Baynes JW (1991) Perspectives in diabetes: role of oxidative stress in development of complications in diabetes. Diabetes 40: 405–412
11. Horie K, Miyata T, Maeda K, Miyata S, Sakai H, Ypersele de Strihou C van, Monnier VM, Wiztum JL, Kurokawa K (1997) Immunohistochemical colocalization of glycoxidation products and lipid peroxidation products in diabetic renal glomerular lesions: implication for glycoxidative stress in the pathogenesis of diabetic nephropathy. J Clin Invest 100: 2995–3004
12. Miyata T, Wada Y, Cai Z, Iida Y, Horie K, Yasuda Y, Maeda K, Kurokawa K, Ypersele de Strihou C van (1997) Impication of an increased oxidative stress in the formation of advanced glycation end products in patients with end-stage renal failure. Kidney Int 51: 1170–1181
13. Li JJ, Surini M, Catsicas S, Kawashima E, Bouras C (1995) Age-dependent accumulation of advanced glycosylation end products in human neurons. Neurobiol Aging 16: 69–76
14. Kimura T, Takamatsu J, Araki N, Goto M, Kondo A, Miyakawa T, Horiuchi S (1996) Accumulation of advanced glycation end products of the Maillard reaction with age in human hippocampal neurons. Neurosci Lett 208: 53–56
15. Vitek MP, Bhattacharya K, Glendening M, Stopa E, Vlassara H, Bucala R, Manogue K, Cerami A (1994) Advanced glycation end products contribute to amyloidosis in Alzheimer disease. Proc Natl Acad Sci USA 91: 4766–4770
16. Yan SD, Chen X, Schmidt AM, Brett J, Godman G, Zou YS, Scott CW, Caputo C, Frappier T, Smith MA, Perry G, Yen SH, Stern D (1994) Glycated tau protein in Alzheimer disease: a mechanism for induction of oxidant stress. Proc Natl Acad Sci USA 91: 7787–7791
17. Smith MA, Taneda S, Richey PL, Miyata S, Yan SD, Stern D, Sayre LM, Monnier VN, Perry G (1994) Advanced Maillard reaction end products are associated with Alzheimer disease pathology. Proc Natl Acad Sci USA 91: 5710–5714
18. Takeda A, Yasuda T, Miyata T, Mizuno K, Li M, Yoneyama S, Horie K, Maeda K, Sobue G (1996) Immunohistochemical study of advanced glycation end products in aging and Alzheimer's disease brain. Neurosci Lett 221: 17–20
19. Horie K, Miyata T, Yasuda T, Takeda A, Yasuda Y, Maeda K, Sobue G, Kurokawa K (1997) Immunohistochemical localization of advanced glycation end products, pentosidine and carboxymethyllysine in lipofuscin pigments of Alzheimer's disease and aged neurons. Biochem Biophys Res Commun 236: 327–332
20. Takeda A, Yasuda T, Miyata T, Goto Y, Wakai M, Watanabe M, Yasuda Y, Horie K, Inagaki T, Doyu M, Maeda K, Sobue G (1998) Advanced glycation end products co-localized with astrocytes and microglial cells in Alzheimer's disease brain. Acta Neuropahol 95: 555–558
21. Yan SD, Chen X, Fu J, Chen M, Zhu H, Roher A, Slattery T, Zhao L, Nagashima M, Morser J, Migheli A, Nawroth P, Stern D, Schmidt AM (1996) RAGE and amyloid-β peptide neurotoxicity in Alzheimer's disease. Nature 382: 685–691
22. Sasaki N, Fukatsu R, Tsuzuki K, Hayashi Y, Yoshida T, Fujii N, Koike T, Wakayama L, Yanagihara R, Garruto R, Amano N, Makita Z (1998) Advanced glycation end products in Alzheimer's disease and other neurodegenerative diseases. Am J Pathol 153: 1149–1155
23. Mattson MP, Carney JW, Butterfield DA (1995) A tombstone in Alzheimer's? Nature 373: 481
24. Liu Y, Dargusch R, Schubert D (1997) Beta amyloid toxicity does not require RAGE protein. Biochem Biophys Res Commun 237: 37–40
25. Kume S, Takeya M, Mori T, Araki N, Suzuki H, Horiuchi S, Kodama T, Miyauchi Y, Takahashi K (1995) Immunohistochemical and ultrastructural detection of advanced glycation end products in atherosclerotic lesions of human aorta using a novel specific monoclonal antibody. Am J Pathol 147: 654–667
26. Ikeda K, Higashi T, Sano H, Jinnouchi Y, Yoshida M, Araki T, Ueda S, Horiuchi S (1996) *N*ε-(Carboxymethyl)lysine protein adducts is a major immunological epitope in proteins modified with advanced glycation end products of the Maillard reaction. Biochemistry 35: 8075–8083
27. Kimura T, Takamatsu J, Miyata T, Miyakawa T, Horiuchi S (1998) Localization of identified advanced glycation end-product structures, *N*ε-(carboxymethyl)lysine and pentosidine, in age-related inclusions in human brains. Pathol Int 48: 575–579
28. Li M, Miwa S, Kobayashi Y, Merry DE, Yamamoto M, Tanaka F, Doyu M, Hashizume Y, Fischbeck KH, Sobue G (1998) Nuclear inclusions of androgen receptor protein in spinal and bulbar muscular atrophy. Ann Neurol 44: 249–254
29. Li M, Nakagomi Y, Kobayashi Y, Merry DE, Tanaka F, Doyu M, Mitsuma T, Hashizume Y, Fischbeck KH, Sobue G (1998) Nonneural nuclear inclusions of androgen receptor protein in spinal and bulbar muscular atrophy. Am J Pathol 153: 695–701
30. Markesbery WR (1997) Oxidative stress hypothesis in Alzheimer's disease. Free Radic Biol Med 23: 134–147
31. Good PF, Werner P, Hsu A, Olanow CW, Perl DP (1996) Evidence for neuronal oxidative damage in Alzheimer's disease. Am J Pathol 149: 21–28
32. Smith MA, Perry G, Richey PL, Sayre LM, Anderson VE, Beal MF, Kowall N (1996) Oxidative damage in Alzheimer's. Nature 382: 120–121
33. Wilson JX (1997) Antioxidant defense of the brain: a role for astrocytes. Can J Physiol Pharmacol 75: 1149–1163
34. Desagher S, Glowinski J, Premont J (1996) Astrocytes protect neurons from hydrogen peroxide toxicity. J Neurosci 16: 2553–2562
35. Pechan PA, Chowdhury K, Seifert W (1992) Free radicals induce gene expression of NGF and bFGF in rat astrocyte culture. NeuroReport 3: 469–472
36. Montine KS, Reich E, Neely D, Sidell KR, Olson SJ, Markesbery WR, Montine TJ (1998) Distribution of reducible 4-hydroxynoneal adduct immunoreactivity in Alzheimer disease is associated with APOE genotype. J Neuropathol Exp Neurol 57: 415–425
37. Doi T, Vlassara H, KirsteinM, Yamada Y, Striker GE, Striker LJ (1992) Receptor-specific increase in extracellular matrix production in mouse mesengial cells by advanced glycosylation end products is mediated via platelet-derived growth factor. Proc Natl Acad Sci USA 89: 2873–2877
38. Hayase F, Kato H (1994) Maillard reaction products: safety and physiologic effects. Comments on Agric Food Chem 3: 111–128

39. Okado A, Kawasaki Y, Hasuike Y, Takahashi M, Teshima T, Fujii J, Taniguchi N (1996) Induction of apoptotic cell death by methylglyoxal and 3-deoxyglucosone in macrophage-derived cell lines. Biochem Biophys Res Commun 225: 219–224
40. Stojanovic A, Roher AE, Ball MJ (1994) Quantitative analysis of lipofuscin and neurofibrillary tangles in the hippocampal neurons of Alzheimer disease brains. Dementia 5: 229–233
41. Jolly RD, Dalefoeld RR, Palmer DN (1993) Ceroid, lipofuscin and the ceroid-lipofuscinosis (Batten disease). J Inherit Dis 16: 280–283
42. Fu MX, Requena JR, Jenkins AJ, Lyons TJ, Baynes JW, Thrope SR (1996) The advanced glycation end product, N^{ε}-(carboxymethyl)lysine, is a product of both lipid peroxidation and glycoxidation reactions. J Biol Chem 271: 9982–9986
43. Castellani R, Smith MA, Richey PL, Perry G (1996) Glycoxidation and oxidative stress in Parkinson disease and diffuse Lewy body disease. Brain Res 737: 195–200
44. Munch G, Cunningham AM, Riederer P, Braak E (1998) Advanced glycation endproducts are associated with Hirano bodies in Alzheimer's disease. Brain Res 796: 307–310
45. Shibata N, Hirano A, Kato S, Nagai R, Horiuchi S, Komori T, Umahara T, Asayama K, Kobayashi M (1999) Advanced glycation endproducts are deposited in neuronal hyaline inclusions: a study on familial amyotrophic lateral sclerosis with superoxide dismutase-1 mutation. Acta Neuropathol 97: 240–246
46. Kato S, Horiuchi S, Nakashima K, Hirano A, Shibata N, Nakano I, Saito M, Kato M, Asayama K, Ohama E (1999) Astrocytic hyaline inclusions contain advanced glycation endproducts in familial amyotrophic lateral sclerosis with superoxide dismutase 1 gene mutation: immunohistochemical and immunoelectron microscopical analyses. Acta Neuropathol 97: 260–266